

Phytoplankton thermal responses adapt in the absence of hard thermodynamic constraints

Dimitrios - Georgios Kontopoulos^{1,2,*}, Erik van Sebille^{3,4}, Michael Lange⁵,
Gabriel Yvon-Durocher⁶, Timothy G. Barraclough², and Samraat Pawar²

1. Science and Solutions for a Changing Planet DTP;

2. Department of Life Sciences, Imperial College London, Silwood Park, Ascot, Berkshire
SL5 7PY, UK;

3. Grantham Institute, Imperial College London, London SW7 2AZ, UK;

4. Institute for Marine and Atmospheric Research Utrecht, Utrecht University, Utrecht
3584 CC, the Netherlands;

5. Department of Earth Science and Engineering, Imperial College London, London SW7
2AZ, UK;

6. Environment and Sustainability Institute, University of Exeter, Penryn, Cornwall
TR10 9EZ, UK;

* Corresponding author; e-mail: d.kontopoulos13@imperial.ac.uk.

Abstract

To better predict how populations and communities respond to climatic temperature variation, it is necessary to understand how the shape of the response of fitness-related traits to temperature evolves (the thermal performance curve). Currently, there is disagreement about the extent to which the evolution of thermal performance curves is constrained. One school of thought has argued for the prevalence of thermodynamic constraints through enzyme kinetics, whereas another argues that adaptation can—at least partly—overcome such constraints. To shed further light on this debate, we perform a phylogenetic meta-analysis of the thermal performance curve of growth rate of phytoplankton—a globally important functional group—, controlling for potential environmental effects. We find that thermodynamic constraints have a minor influence on the shape of the curve. In particular, we detect a very weak increase of the maximum curve height with the temperature at which the curve peaks, suggesting a weak “hotter-is-better” constraint. Also, instead of a constant thermal sensitivity of growth across species, as might be expected from strong constraints, we detect phylogenetic signal in this as well as all other curve parameters. Our results suggest that phytoplankton thermal performance curves adapt to thermal environments largely in the absence of hard thermodynamic constraints.

Keywords

Thermal response, phytoplankton, thermal adaptation, constraints, growth rate, trait.

Introduction

Temperature changes can affect the dynamics of all levels of biological organization by changing the metabolic rate of individual organisms (Brown et al., 2004; Pörtner et al., 2006; Hoffmann and Sgrò, 2011; Pawar et al., 2015). Thus, to better understand the impacts of current and future climate change on whole ecosystems, it is essential to understand how key fitness-related metabolic traits (e.g., growth rate, photosynthesis rate) respond to changes in environmental temperature.

In ectotherms, the relationship of fitness-related traits with temperature (the “thermal performance curve”; TPC) is typically unimodal (Fig. 1; Angilletta 2009). Trait values increase with temperature until a critical point (T_{pk}), after which they drop rapidly. To understand the capacity for adaptation of the TPC to different thermal environments, it is important to investigate how the shape of the TPC evolves across species. This remains an area of ongoing debate, with multiple competing hypotheses existing in the literature. Such hypotheses can be broadly classified along a continuum that ranges from strong and insurmountable constraints on TPC evolution due to thermodynamic constraints on enzyme kinetics, to weak constraints that can be overcome through adaptation (Fig. 2).

At the strong thermodynamic constraints extreme, the “hotter-is-better” hypothesis (Frazier et al., 2006; Knies et al., 2009; Angilletta et al., 2009; Angilletta, 2009) posits that TPCs evolve under severe constraints, due to the impact of thermodynamics on enzyme kinetics. More precisely, hotter-is-better predicts that a rise in the peak temperature (T_{pk}) through adaptation to a hotter environment will necessarily lead to an increase in the maximum height of the curve (B_{pk}). The increase in B_{pk} is assumed to be the outcome of the acceleration of enzyme reactions as temperature rises. It is worth clarifying that hotter-is-better only refers to the relationship of B_{pk} with T_{pk} , and does not posit that growth rate can increase indefinitely with temperature in any one species’ TPC (Fig. 2A). Hotter-is-better is implicit in the Metabolic Theory of Ecology (MTE; Brown et al. 2004). MTE also predicts that the performance of metabolic traits is linked with body size (e.g., temperature-normalised pop-

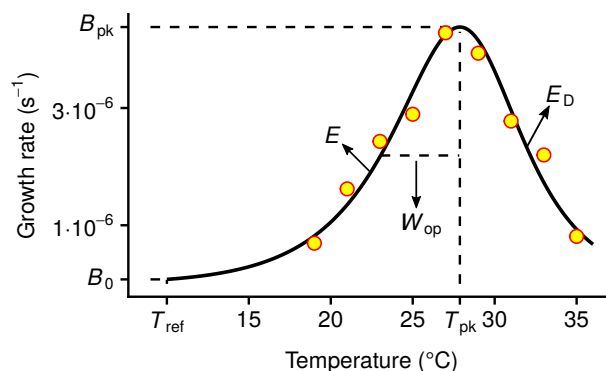


Figure 1. The relationship of growth rate (r_{\max}) with temperature in ectotherms (the thermal performance curve; TPC). The TPC is generally unimodal and asymmetric, here quantified by the four-parameter Sharpe-Schoolfield model (black line; Schoolfield et al. 1981) fitted to growth rate measurements of the dinoflagellate *Amphidinium klebsii* (Morton et al., 1992). The parameters of the model are B_0 (in units of s^{-1}), E (eV), T_{pk} (K), and E_D (eV). B_0 is the growth rate at a reference temperature below the peak (T_{ref}) and controls the vertical offset of the TPC. E sets the rate at which the curve rises and is, therefore, a measure of thermal sensitivity at the operational temperature range. T_{pk} is the temperature at which growth rate is maximal, and E_D controls the fall of the curve. Two other parameters control the shape of the curve and can be calculated from the four main parameters: B_{pk} (s^{-1}); the maximum height of the curve, and W_{op} (K); the operational niche width, which we define as the difference between T_{pk} and the temperature at the rise of the curve where growth rate is half of B_{pk} .

ulation growth rate scales negatively with mass). Thus, adaptation to a high-temperature environment would not only lead to an increase in the maximum trait performance (B_{pk}), but also to a decrease in body size. In its strictest form (Fig. 2A), hotter-is-better makes a number of strong and likely unrealistic assumptions. First, because of thermodynamic constraints, E (a measure of thermal sensitivity; Fig. 1) is expected to vary very little across species, with negligible capacity for environmental adaptation (Gillooly et al., 2006). Second, under a strict hotter-is-better scenario, if B_0 is calculated at a low enough normalisation

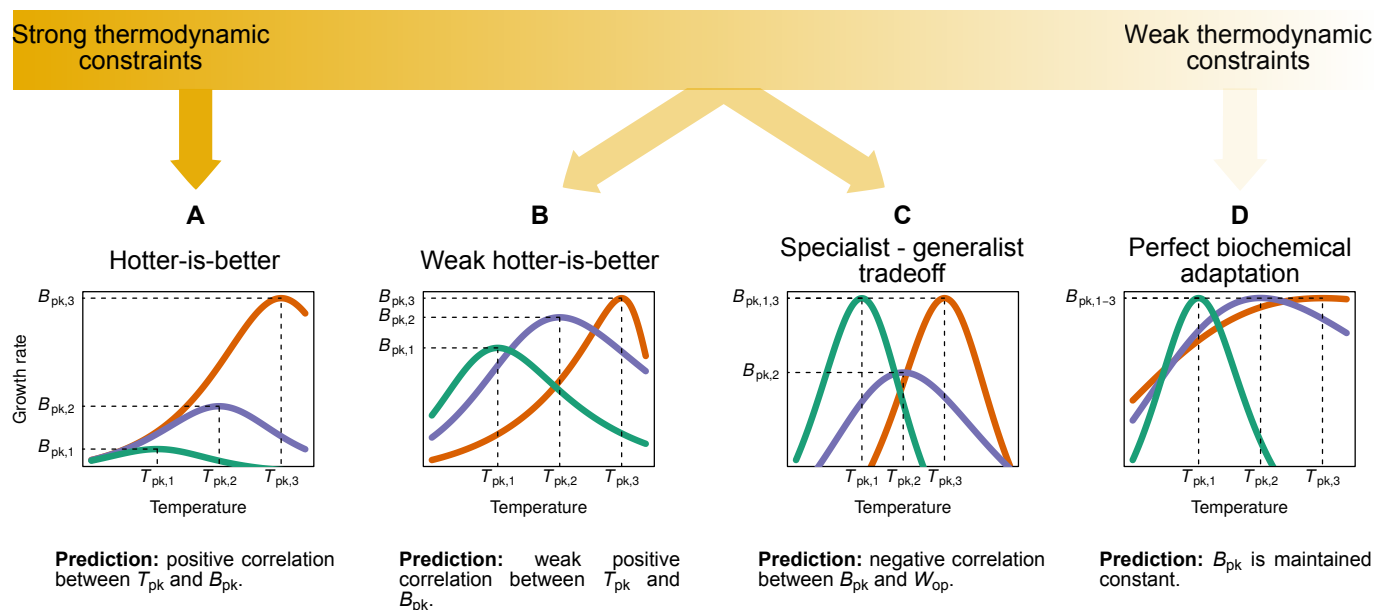


Figure 2. The spectrum of hypotheses for the evolution of thermal performance curves across species. A key area of difference among these hypotheses concerns the impact of thermodynamic constraints on the shape of the TPC. Thus, hypotheses can be classified between those lying near the strong thermodynamic constraints end, the middle of the spectrum, or the weak thermodynamic constraints end where thermodynamic constraints can be overcome through biochemical adaptation. It is worth clarifying that in panel D, the maximum value that B_{pk} can take would also be under a thermodynamic constraint, but this constraint would be different from those assumed in panels A and B. A detailed description of each hypothesis is provided in the main text.

temperature (T_{ref}), then B_0 is also expected to be invariable across species (see Fig. 2A).

This also implies that the body size-scaling of growth rate predicted by MTE must occur at temperatures close to the peak of the curve and not at a low T_{ref} (otherwise, B_0 would vary because of size-growth rate scaling, in contrast to the scenario shown in Fig. 2A).

Relaxing at least one of these assumptions of the strict hotter-is-better hypothesis (e.g., if adaptation can be traced in E or B_0 at a low T_{ref}) leads to a more realistic weak hotter-is-better hypothesis (Fig. 2B), located near the middle of the spectrum. Indeed, recent work has shown that significant variation in E exists within and across species, suggesting that this variation is likely adaptive (Dell et al., 2011; Nilsson-Örtman et al., 2013; Pawar et al., 2016; García-Carreras et al., 2018). Under weak hotter-is-better, growth rate is still expected to increase with temperature but the correlation between T_{pk} and B_{pk} should be weaker. Another hypothesis that lies in the middle of the spectrum is the specialist-generalist tradeoff hypothesis (Huey and Hertz, 1984; Angilletta, 2009). This hypothesis suggests that there is a tradeoff between maximum trait performance (B_{pk}) and thermal niche width (W_{op}). That is, a widening of the niche necessarily incurs a metabolic cost, leading to a decrease in peak performance (Fig. 2C). It is worth mentioning that the weak hotter-is-better and the specialist-generalist tradeoff hypotheses are not mutually exclusive, as their predictions stem from very different mechanisms which could potentially interact.

At the other end of the spectrum lie a class of hypotheses which posit that the influence of thermodynamic constraints should be reduced or minimised through adaptation of species' biochemical machinery (Hochachka and Somero, 2002; Clarke and Fraser, 2004; Angilletta, 2009; Clarke, 2017). An extreme example is the “perfect biochemical adaptation” hypothesis, which posits that adaptation should allow species to maximise their performance (B_{pk}) in any thermal environment (Fig. 2D) by overcoming biochemical constraints. Nevertheless, an upper limit to the maximum possible B_{pk} across species or evolutionary lineages would still be present, but due to a different thermodynamic constraint from that expected under hotter-is-better. While some studies have found support for the perfect biochemical adaptation

hypothesis (e.g., for TPCs of gross photosynthesis rate; Padfield et al. 2016, 2017), it remains
 96 unclear whether species can always reach the global maximum in B_{pk} , or rather a local
 maximum that varies across different environments.

The above hypotheses are not an exhaustive list but lie on a spectrum (Fig. 2). To
 99 understand the position of different metabolic traits and/or species groups on this spectrum,
 it is necessary to investigate i) the correlations between multiple thermal parameters and ii)
 how each thermal parameter evolves across species. A basic understanding of the latter can
 102 be obtained by measuring the phylogenetic signal in each TPC parameter, i.e., the extent
 to which closely related species are more similar to each other than to any species chosen
 at random (Pagel, 1999; Kamilar and Cooper, 2013; Symonds and Blomberg, 2014). Strong
 105 phylogenetic signal would indicate that variation in the TPC parameter can be explained
 by its gradual evolution across the phylogeny. On the other hand, a lack of phylogenetic
 signal would reflect either trait stasis (with any variation among species being noise-like) or
 108 very rapid evolution (that is independent of the phylogeny and cannot be traced on it). In
 both cases, closely related species would not be more similar in their TPC parameter values
 than randomly selected species. This pattern can be modelled using a white noise process.
 111 Intermediate values of phylogenetic signal would imply either that the TPC parameter is
 under constrained evolution (e.g., due to stabilizing selection), or that its evolutionary rate
 changes through time (e.g., decelerating after an adaptive radiation or accelerating as the
 114 niches of distantly related species converge).

To the best of our knowledge, a thorough analysis of the correlation structure among
 parameters that control the entire range of the TPC has never been conducted. At most,
 117 previous studies have investigated the existence of correlations between two or three selected
 TPC parameters (e.g., between T_{pk} and B_{pk} ; see Frazier et al. 2006 and Sørensen et al.
 2018). This can be problematic for two reasons. First, by only focusing on parameters that
 120 control the peak of the TPC, such studies ignore potential correlations with parameters in
 other areas of the curve (e.g., E). Second, even if a statistical correlation can be observed

between two thermal parameters, it may potentially be driven by the covariance of the two parameters with other, overlooked parameters of the TPC. Indeed, many studies on TPCs do not explicitly account for phylogenetic relationships among species at all (but see Sal et al. 2015 for a phylogenetically-controlled study on the size-scaling of phytoplankton growth rate). Ignoring potential phylogenetic effects can make it harder to differentiate between alternative hypotheses on the evolution of TPCs, and may leave studies vulnerable to biases introduced by phylogenetic nonindependence (e.g., an observed relationship between two TPC parameters could arise solely from uneven phylogenetic sampling).

Taking these issues into consideration, here we investigate the evolution of the TPC of a fundamental measure of fitness—population growth rate (r_{\max})—using a global database of phytoplankton measurements. We chose phytoplankton as a study system for ecological and practical reasons. First, phytoplankton form the autotroph base of most aquatic food webs and contribute around half of the global primary production (Field et al., 1998). Second, phytoplankton are one of the few species groups for which sufficiently large TPC datasets are available.

Within phytoplankton, we also explore whether the impact of thermodynamic constraints on the shape of the TPC varies between freshwater and marine species. In particular, as freshwater phytoplankton have a limited potential for dispersal, the timescale of temperature fluctuations that they experience can be quite different from that of marine phytoplankton which are passively moved by ocean currents across large distances (Doblin and van Sebille, 2016). Such intricacies of the marine environment could potentially be reflected in the TPCs of marine species.

Methods

To understand whether and how thermodynamic constraints influence the evolution of the shape of TPCs of phytoplankton, here we analyse the correlations between TPC parameters

both within and across species. For the latter, we take a phylogenetic comparative approach which allows us to partition the covariance between six TPC parameters of phytoplankton into a phylogenetically heritable component, a fixed effects component (covariance due to environmental effects that were controlled for), and a residual component. To this end, we estimate the amount of heritable covariance by building a phylogeny of the species in our dataset and combining it with multi-response regression models. We also simultaneously control for the environment from which species/strains were isolated. For marine species in particular, we simulate the trajectories of drifting marine phytoplankton to get realistic estimates of the temperatures that they experience through drifting.

Data

We compiled a global database on growth rate performance of phytoplankton species by combining the previously published datasets of López-Urrutia et al. (2006), Rose and Caron (2007), Bissinger et al. (2008), and Thomas et al. (2012). Growth rates across temperatures were typically measured under light- and nutrient-saturated conditions in these studies. Species names were standardised by querying the Encyclopedia of Life (Parr et al., 2014) via the Global Names Resolver (Global Names Architecture, 2017), followed by manual inspection. This ensured that synonymous species names were represented under a common name. From 795 original species/strain names, this process yielded 380 unique taxa from nine phyla. Where multiple strains of the same species (or isolates from different locations) were available, we did not perform any averaging of growth rate measurements, but analyzed each isolate separately. This allowed us to capture both the inter- and intraspecific variation, where possible. The isolation locations of species/strains in the dataset ranged in latitude from 78°S to 80°N (Fig. S1 in the Supporting Information (SI)).

For cell volume data, those available from original studies were combined with median volume measurements reported by Kremer et al. (2014). This process resulted in a dataset with cell volumes for most phytoplankton TPCs, spanning seven orders of magnitude.

Estimation of TPC parameter values

To quantify all key features of the shape of each growth rate TPC, we used a modified formulation (with T_{pk} as an explicit parameter; SI section S2.1) of the four-parameter variant of the Sharpe-Schoolfield model (Schoolfield et al. 1981; Fig. 1):

$$B(T) = B_0 \cdot \frac{e^{\left[\frac{-E}{k} \cdot \left(\frac{1}{T} - \frac{1}{T_{ref}} \right) \right]}}{1 + \frac{E}{E_D - E} \cdot e^{\left[\frac{E_D}{k} \cdot \left(\frac{1}{T_{pk}} - \frac{1}{T} \right) \right]}}. \quad (1)$$

Here, the growth rate, B (s^{-1}), at a given temperature T (K) is expressed as a function of four parameters (B_0 , E , E_D and T_{pk} ; see Fig. 1 for their description and units), and the Boltzmann constant, k ($8.617 \cdot 10^{-5}$ eV \cdot K $^{-1}$). The key assumption of this model is that growth rate is controlled by a single rate-limiting enzyme which is deactivated at high temperatures, whereas, at low temperatures, it operates at a decreased rate because of the low available kinetic energy. Whether this assumption is justified remains under debate (e.g., see Gillooly et al. 2001; Clarke and Fraser 2004; Clarke 2004; Gillooly et al. 2006; Clarke 2006, 2017). Nevertheless, we chose this model for two reasons. First, from a statistical point of view, the model adequately captures the relationship between growth rate and temperature. Second, the mathematical structure of the model is based on principles of enzyme thermodynamics and, as a result, some of the asymptotic correlations among the parameters of the model (see next subsection) reflect the strength of thermodynamic constraints. Thus, basing the analysis on the Sharpe-Schoolfield model allows for directly examining the influence of different thermodynamic constraints on TPC evolution. Such an analysis would not be possible with a phenomenological model.

We fitted the Sharpe-Schoolfield model separately to each species/strain in the dataset, using the Levenberg-Marquardt nonlinear least squares minimization algorithm (SI section S2.2). After obtaining estimates of the four main model parameters, we used them to calculate the values of two more parameters: i) B_{pk} , and ii) W_{op} (K) (Fig. 1).

For a correct comparison of B_0 estimates, T_{ref} needs to be set lower than the minimum T_{pk} in the dataset (otherwise, for certain TPCs, B_0 is estimated at the fall of the curve instead of the rise, and the comparison becomes meaningless). As there were a few fits with T_{pk} values close to 0°C , we set T_{ref} to 0°C . However, to ensure that a performance comparison at 0°C does not bias the results of this study—given that some species may not tolerate that low a temperature—, we also fitted the Sharpe-Schoolfield model using a T_{ref} of 10°C . In that case, we excluded fits with $T_{\text{pk}} < 10^\circ\text{C}$. All subsequent analyses were performed using both datasets (i.e., those obtained with a T_{ref} of 0°C and 10°C), to identify potential areas of disagreement. Finally, as the estimate of B_0 from the Sharpe-Schoolfield model can sometimes strongly deviate from the true rate value ($B(T_{\text{ref}})$) depending—among others— on the choice of T_{ref} (Kontopoulos et al., 2018), we calculated $B(T_{\text{ref}})$ manually after fitting (henceforth referred to as B_0).

Quality filtering of the fits resulted in a TPC dataset of 270 curves using a T_{ref} of 0°C and of 259 curves using a T_{ref} of 10°C (SI Figs. S2 and S3).

Quantifying correlations among parameters of intraspecific TPCs

We first evaluated thermodynamic constraints on each species' TPC by estimating the correlation between its parameters. As mentioned above, covariances between parameter pairs of the Sharpe-Schoolfield model are not purely phenomenological (as are, for example, the covariances between the parameters of a polynomial equation) but have thermodynamic interpretations. If thermodynamic constraints were ubiquitous, we would expect to find strong correlations among the parameters of the Sharpe-Schoolfield model, whereas the correlation coefficients would be nearly identical across species.

We obtained these species-level TPC parameter correlations from the asymptotic variance/covariance matrix estimated during the NLLS model fitting for each TPC (see Schoolfield et al. 1981). This matrix is obtained by calculating the partial derivatives of the Sharpe-Schoolfield model, i.e., by slightly perturbing one parameter estimate at a time and observing

how the remaining parameter estimates change in response. The off-diagonal elements of the variance/covariance matrix are the pairwise parameter covariances, from which the asymptotic correlations can be calculated. For this analysis, we selected the highest quality fits across our dataset, i.e., those which passed our filtering criteria (SI section S2.2), and which had at least four experimentally measured data points both at the rise and at the fall of the curve. This led to a smaller dataset of 30 TPCs.

Reconstruction of the phytoplankton phylogeny

To our knowledge, there was no publicly available phylogenetic tree that includes all the phytoplankton phyla and species in our TPC dataset. Therefore, we reconstructed their phylogeny using nucleotide sequences of the small subunit rRNA gene (see Table S21 in the SI). One sequence was collected per species where possible, resulting in a dataset of 138 nucleotide sequences. Given that increased taxon sampling has been shown to improve the quality of phylogenetic trees (Nabhan and Sarkar, 2012; Wiens and Tiu, 2012), we also collated a second dataset of 323 sequences by expanding the previous dataset with further sequences of phytoplankton, macroalgae, and land plants. The two sets of nucleotide sequences were aligned with MAFFT (v7.123b; Katoh and Standley 2013), using the L-INS-i algorithm. We then used the entire alignments to build phylogenetic trees without masking any columns, as this has been shown to occasionally result in worse topologies when only a single gene is used (Tan et al., 2015).

Tree topologies were inferred with RAxML (v. 8.2.4; Stamatakis 2014), PhyML (v. 20151210; Guindon et al. 2010), and ExaBayes (v. 1.4.1; Aberer et al. 2014), under the General Time-Reversible model (Tavaré, 1986) with Γ -distributed rate variation among sites (four discrete rate categories; Gu et al. 1995). For RAxML, in particular, we inferred 300 distinct topologies using the slow hill-climbing algorithm (which performs a more thorough exploration of likelihood space than the default algorithm; option “-f o”), and selected the tree topology with the highest log-likelihood. For PhyML we used the default options, with

the exception of the topology search which was set to include both the Nearest Neighbor Interchange (NNI) and the Subtree Pruning and Regrafting (SPR) procedures. For ExaBayes, we executed four independent runs with four Metropolis-coupled chains per run for 55 million generations. Samples from the posterior distribution were obtained every 500 generations, after discarding the first 25% of samples as burn-in. We confirmed that the four ExaBayes runs had converged through a range of tests (see sections S3.1 and S3.2 in the SI), and obtained a tree topology by computing the extended majority-rule consensus tree. The best tree topology—among those produced by RAxML, PhyML, and ExaBayes—was selected on the basis of proximity to the Open Tree of Life (Hinchliff et al., 2015), and log-likelihood (SI section S3.3).

We then estimated relative ages for all nodes of the best topology, using the uncorrelated Γ -distributed rates model (Drummond et al., 2006), as implemented in DPPDiv (Heath et al., 2012; Flouri and Stamatakis, 2012). To this end, we executed five independent runs for 750,000 generations, sampling from the posterior distribution every 100 generations. As before, we discarded the first 25% of samples as burn-in, and performed diagnostic tests to ensure that the posterior distributions of the four runs had converged and that the parameters were adequately sampled (SI section S3.4). To obtain the final relative time-calibrated tree, we sampled every 300th tree from each run (after the burnin phase) for a total of 9,375 trees, and calculated the median age estimate for each node using the TreeAnnotator program (Rambaut and Drummond, 2017).

Modelling the local thermal environments of marine phytoplankton

As mentioned previously, although marine phytoplankton are passively moved by ocean currents across large distances, little attention has been given to the potential effects of this on their thermal physiology. In particular, Doblin and van Sebille (2016) showed that the temperature range that marine microbes likely experience is usually much wider if oceanic drifting is properly accounted for. Therefore, to accurately quantify the thermal regimes

of marine phytoplankton, we simulated Lagrangian (drifting) trajectories with the Python package OceanParcels (Lange and van Sebille, 2017). More precisely, we used hydrodynamic data from the OFES model (ocean model for the Earth Simulator; Masumoto et al. 2004) to estimate 3,770 backwards-in-time replicate trajectories for each marine location in the dataset over 500 days (using a one-day timestep), at a depth of 2.5, 50, or 100 meters (where possible). These depth values were chosen after considering global estimates of oceanic euphotic depth (Morel et al., 2007), i.e. the depth below which net primary production by marine autotrophs becomes negative (Falkowski and Raven, 2013).

We then calculated the following environmental variables: i) the median temperature experienced, ii) the median latitude visited, iii) the interquartile range of temperatures, and iv) the interquartile range of latitudes. The median captures the central tendency of the temperatures or latitudes that phytoplankton experienced, whereas the interquartile range is a measure of deviation from the central tendency. Measuring all four variables is important, as each of them may have a different effect on the shape of the TPC. The values of the variables were first calculated for each trajectory over the full duration of 500 days, but also over the first 350, 250, 150, and 50 days. They were then averaged across all replicate trajectories per location, depth, and duration, weighted by the length of the trajectory, as some trajectories could be estimated for fewer than 500 days. These variables are hereafter referred to as $\tilde{T}_{d,t}$ (median temperature), $\tilde{L}_{d,t}$ (median latitude), $IQR(T_{d,t})$ (interquartile range of temperatures), and $IQR(L_{d,t})$ (interquartile range of latitudes), where d and t stand for the depth and duration of the trajectory respectively.

We also obtained temperature data of the isolation locations of marine phytoplankton, in order to compare their explanatory power with that of the Lagrangian trajectory variables. To this end, we used the NOAA Optimum Interpolation Sea Surface Temperature dataset, which comprises daily measurements of sea surface temperature at a global scale and at a resolution of $1/4^\circ$ (Banzon et al., 2016). Currently, two variants of this dataset are available: i) “AVHRR-Only” which is primarily based on the Advanced Very High Resolution

Radiometer, and ii) “AVHRR+AMSR” which also uses data from the Advanced Microwave Scanning Radiometer on the Earth Observing System. The latter variant is considered more accurate, but, for technical reasons, is only available from 2002 until 2011, whereas the former variant is available from 1981 until the present day. In our case, we obtained a daily sea surface temperature dataset between the 1st of September 1981 and the 25th of June 2017, using AVHRR-Only, or AVHRR+AMSR when that was available. From this dataset, we calculated the median temperature of each marine location (\tilde{T}_{orig}), and the interquartile range of temperatures ($\text{IQR}(T_{\text{orig}})$).

Inference of TPC parameter co-evolution and associations with environmental variables

I. Across the entire dataset

To infer the interspecific correlation structure among the parameters of the TPC and simultaneously detect associations with the local environment of the species in our study, we fitted phylogenetic Markov Chain Monte Carlo generalised linear mixed models using the R package MCMCglmm (v. 2.24; Hadfield 2010). This package can be used to fit phylogenetic regression models, enabling the partitioning of phenotypic trait variance into a phylogenetically heritable component, a fixed effects component of explanatory variables, and a residual variance component (i.e., variance that should be mostly due to environmental effects that are not already controlled for). For the purposes of this study, we constructed multi-response regression models (i.e., models with multiple response variables instead of one), in which the response comprised all six TPC parameters. In other words, instead of trying to predict a single response variable, the models would predict all six TPC parameters, while simultaneously inferring their variance/covariance matrix. Each element of this matrix was independently estimated from the data, so that any correlations between pairs of TPC parameters could be detected.

To ensure that the distribution of each response variable was as close to normality as possible, we applied a different transformation to each TPC parameter: $\sqrt[4]{B_0}$, $\ln(E)$, T_{pk}^2 , $\ln(B_{pk})$, $\ln(E_D)$, $\ln(W_{op})$. It was necessary to perform those transformations as each response variable in an MCMCglmm needs to conform to one of the implemented distributions in the package (e.g., Gaussian, Poisson, multinomial), with the Gaussian distribution being the most appropriate here. Besides this, most macroevolutionary models assume that the evolutionary change in trait values follows a Gaussian distribution. Thus, statistical transformations of trait values are often used to satisfy this assumption. In any case, applying these transformations does not affect our results qualitatively even though thermal parameter correlations are estimated in transformed (not linear) scale. To incorporate the uncertainty for each transformed thermal parameter estimate, we used the delta method (e.g., see Oehlert 1992) implemented in the R package *msm* (v. 1.6.4; Jackson 2011) to obtain appropriate estimates of the variance of the standard error for $\sqrt[4]{B_0}$, $\ln(E)$, T_{pk}^2 , $\ln(B_{pk})$, and $\ln(E_D)$. As we manually calculated $\ln(W_{op})$ a posteriori without an analytical solution, we performed bootstrapping to obtain error estimates for it.

For the majority of the TPCs in our dataset, there was at least one parameter whose value could not be estimated with certainty due to lack of adequate experimental measurements (SI section S2.2). MCMCglmm can accommodate such missing values in the response by treating them as “Missing At Random” (MAR; see Hadfield 2010 and de Villemereuil and Nakagawa 2014). Following the MAR assumption, MCMCglmm automatically infers missing values in a response variable from i) the random effects (e.g., from closely related species in a phylogeny), and from ii) non-missing values in other response variables (as long as these variables covary). Estimates obtained through this approach have been shown to be unbiased, as long as missingness in the data is random and not driven by an unmeasured variable (see Nakagawa and Freckleton 2008; Garamszegi and Møller 2011). Applying this method allowed us to include TPC parameter estimates from curves that were only partly well sampled (e.g., only the rise of the curve), increasing the statistical power of the analysis

and reducing the possibility of estimation biases.

The fixed effects component of each candidate model contained at the very minimum a distinct intercept for each response variable. Starting with this, we fitted models with i) no other predictors (the intercepts-only model), ii) the latitude of the isolation location of each species, iii) the habitat of each species (marine vs freshwater), or iv) both latitude and habitat. For models that included latitude as a predictor, we specified either the absolute latitude of the location or a second order polynomial. In any case, we estimated the association of each fixed effect (latitude and/or habitat) with each response variable separately (by inferring distinct coefficients for, e.g., $\ln(E):|\text{latitude}|$, $\ln(B_{pk}):|\text{latitude}|$). It is worth noting that we did not include the temperature of the environment as a fixed effect in these particular models, as there was no reliable temperature dataset with high enough resolution for both marine and freshwater locations. To avoid any potential biases introduced by a combination of two temperature datasets (one for the marine locations and one for the freshwater ones), we instead used latitude as a proxy for temperature.

Species identity was specified as a random effect on the intercepts. To integrate phylogenetic information into the model, we first pruned the phylogeny to the subset of species for which data were available (SI Fig. S13). We next calculated the inverse of the phylogenetic covariance matrix from the phylogenetic tree, including ancestral nodes as this allows for more computationally efficient calculations (Hadfield and Nakagawa, 2010; de Villemereuil and Nakagawa, 2014).

The default prior was used for the fixed effects, whereas for the random effect and the residual variance components, we used a relatively uninformative inverse- Γ prior with shape and scale equal to 0.001 (the lower this number the less informative is the prior). For each model, two chains were run for 100 million generations, sampling from the posterior distribution every 1000 generations after discarding the first 10 million generations as burn-in. Convergence between each pair of chains was verified by calculating the potential scale reduction factor (Gelman and Rubin, 1992; Brooks and Gelman, 1998) for all estimated pa-

rameters (i.e., fixed effects, elements of the phylogenetically heritable and residual matrices),
 and ensuring that it was always lower than 1.1. We also confirmed that the effective sample
 size of all model parameters—after merging samples from the two chains—was greater than
 200, so that the mean could be adequately estimated.

Model selection was done on the basis of the Deviance Information Criterion (DIC;
 Spiegelhalter et al. 2002), averaged across each pair of chains. We excluded models if a
 fixed effect had a 95% Highest Posterior Density (HPD) interval that included zero for every
 single response variable (e.g., if all of $\sqrt[4]{B_0}$:habitat, $\ln(E)$:habitat, T_{pk}^2 :habitat etc. had 95%
 HPD intervals that included zero). In frequentist statistics terms, this is roughly equivalent
 to excluding models whose predictors were not significant for any response variable. To
 evaluate the quality of the best-fitting model, we first calculated the amounts of variance ex-
 plained by fixed (σ_{fixed}^2) and random effects (σ_{random}^2), and the residual variance (σ_{resid}^2). From
 these, we calculated the marginal (R_m^2) and conditional (R_c^2) coefficients of determination,
 as described by Nakagawa and Schielzeth (2013):

$$R_m^2 = \frac{\sigma_{\text{fixed}}^2}{\sigma_{\text{fixed}}^2 + \sigma_{\text{random}}^2 + \sigma_{\text{resid}}^2}, \quad (2)$$

$$R_c^2 = \frac{\sigma_{\text{fixed}}^2 + \sigma_{\text{random}}^2}{\sigma_{\text{fixed}}^2 + \sigma_{\text{random}}^2 + \sigma_{\text{resid}}^2}. \quad (3)$$

Phenotypic correlations between pairs of TPC parameters (r_{phe}) were broken down into their
 phylogenetically heritable (r_{her}) and residual components (r_{res}) by dividing the covariance
 estimate between two parameters by the geometric mean of their variances. These were
 inferred from the best-fitting model in terms of DIC. A phylogenetic heritability estimate for
 each response variable (i.e., the ratio of heritable variance to the sum of heritable and residual
 variance) was obtained from the intercepts-only model, as the addition of fixed effects would
 reduce the residual variance and bias the heritability estimates towards higher values. As
 the phylogeny is integrated with the MCMCglmm, the calculated phylogenetic heritability

estimates are equivalent to Pagel’s λ (Pagel, 1999; Hadfield and Nakagawa, 2010), and reflect the strength of the phylogenetic signal.

II. For the marine subset of the data

To test whether the correlation structure of thermal parameters across the entire phytoplankton dataset differs from that of marine species only, we also performed the above analysis for only the marine species in the dataset. The main difference in the specification of the MCMCglms for marine species was the choice of fixed effects that we used: i) no fixed effects (intercepts-only model), ii) L_{orig} , iii) \tilde{T}_{orig} , iv) $\text{IQR}(T_{\text{orig}})$, v) $\tilde{T}_{\text{orig}} + \text{IQR}(T_{\text{orig}})$, vi) $\tilde{T}_{\text{d}, \text{t}}$, vii) $\text{IQR}(T_{\text{d}, \text{t}})$, viii) $\tilde{T}_{\text{d}, \text{t}} + \text{IQR}(T_{\text{d}, \text{t}})$, ix) $\tilde{L}_{\text{d}, \text{t}}$, x) $\text{IQR}(L_{\text{d}, \text{t}})$, xi) $\tilde{L}_{\text{d}, \text{t}} + \text{IQR}(L_{\text{d}, \text{t}})$. All latitude variables other than $\text{IQR}(L_{\text{d}, \text{t}})$ were specified—in different models—both as a second order polynomial and with absolute values. A second order polynomial was also tested for $\text{IQR}(T_{\text{d}, \text{t}})$ variables to investigate the existence of a quadratic relationship of $\text{IQR}(T_{\text{d}, \text{t}})$ with thermal parameters.

As there was a very large number of MCMCglms to execute (158 pairs of chains), we first ran each of them for 60 million generations. We then checked whether the two chains per model had converged as previously described, and reran the subset that had not converged for 120 million generations. At that point, all pairs of chains converged on statistically indistinguishable posterior distributions. As above, samples from the first 10% generations of each model were discarded as burn-in.

Size-scaling of B_0 and B_{pk}

As a final step for understanding how TPCs evolve, it is necessary to test whether growth rate scales with body size as expected from the Metabolic Theory of Ecology. Under strict hotter-is-better, such scaling would be expected only for growth rates near T_{pk} , whereas if the weak hotter-is-better hypothesis holds, size scaling could also—but not necessarily—occur at low temperatures (near T_{ref}). We investigated these by fitting MCMCglms with

cell volume as a fixed effect and a single response of either i) B_0 (at a T_{ref} of 0°C), ii) B_0 (at a T_{ref} of 10°C), or iii) B_{pk} . Species identity was treated as a random effect on the intercept, the slope, or both. Each model was fitted with and without the phylogenetic variance/covariance matrix to compare the predictions obtained by ignoring the phylogeny or accounting for it. Two chains were run per model for a length of 3 million generations, and convergence was established as in the previous section after removing samples from the first 300,000 generations. DIC was used to identify the most appropriate model for each response variable.

Results

Analysis of asymptotic correlations for each TPC

A remarkable amount of interspecific variation was detected in the distributions of asymptotic correlations between pairs of TPC parameters (Fig. 3). Most parameter pairs exhibit a wide range of correlations, from extreme negative to extreme positive values. This wide diversity suggests that hard thermodynamic constraints are not the primary drivers of the shape of phytoplankton TPCs. The only exception is the correlation between B_0 and E which generally tends to be very close to -1, although in a few cases it becomes weaker. This strong negative correlation indirectly highlights a constraint in the maximum height of the TPC (B_{pk}). In other words, if there is an upper limit in B_{pk} , TPCs are expected to have either a high intercept (B_0) along with a low rising slope (E), or vice versa. Considerable variation in correlations was typically present even within phyla (e.g., within Cyanophyta). However, the sample size was not adequate for a systematic comparison of the correlation space occupied by different phyla.

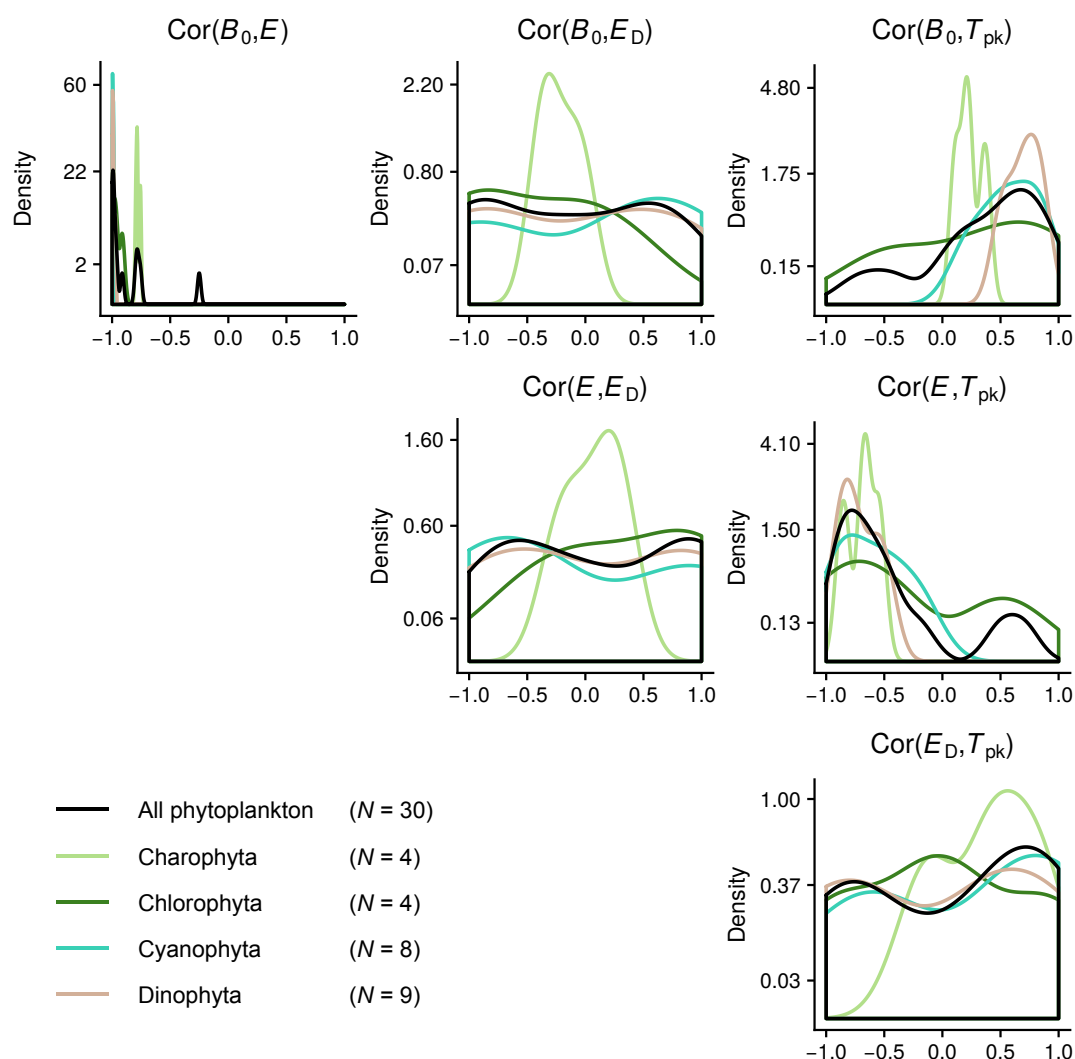


Figure 3. Distributions of asymptotic correlations among the four main TPC parameters, across the best experimentally characterised TPCs in the dataset.

Interspecific correlations and phylogenetic signal

The best-fitting phylogenetic regression model—on the basis of DIC—had only latitude as a fixed effect (SI Figs. S14 and S15). Models with habitat as a predictor were excluded from the DIC comparison, as the 95% Highest Posterior Density interval of every single habitat coefficient included zero. Instead, the 95% HPD intervals of the coefficients of latitude for T_{pk} (for both T_{ref} values) and E (for a T_{ref} of 0°C only) did not include zero (SI Fig. S16). A key difference between the analyses with a T_{ref} of 0°C and 10°C was that in the former case, the model with a second order polynomial in latitude was selected, whereas in the latter case, absolute latitude performed better. The amount of variance explained by latitude was similar across the analyses with the two T_{ref} values: $R_m^2 = 0.516$ and $R_c^2 = 0.999$ for $T_{ref} = 0^\circ\text{C}$, $R_m^2 = 0.507$ and $R_c^2 = 0.999$ for $T_{ref} = 10^\circ\text{C}$. The shapes of the two fitted curves (SI Fig. S16) suggest that the effect of latitude on the TPC is particularly strong for colder-adapted species, leading to a deviation from a strictly linear association.

From the analysis of the resulting interspecific variance/covariance matrices, we identified only two correlations among TPC parameters: i) between B_{pk} and T_{pk} (Fig. 4), and ii) between E and W_{op} (SI Fig. S17). The former correlation appears to be driven entirely by the phylogenetically heritable component of the coldest-adapted species in the dataset, and becomes nonexistent when these are excluded. Such a pattern is consistent with the weak hotter-is-better hypothesis (Fig. 2). Also, as E and W_{op} are both measures of thermal sensitivity near the range of temperatures where organisms typically operate, a negative correlation between them was expected under all TPC evolution hypotheses. Finally, we detected varying amounts of phylogenetic signal in all TPC parameters, with T_{pk} showing the strongest (perfect phylogenetic) signal (Fig. 5). This was in contrast to the assumptions of the strict hotter-is-better and the perfect biochemical adaptation hypotheses, which posit that E and B_{pk} respectively should vary very little across species and not in a phylogenetically heritable manner (Fig. 2).

Running MCMCglms for the marine species only yielded mostly similar conclusions

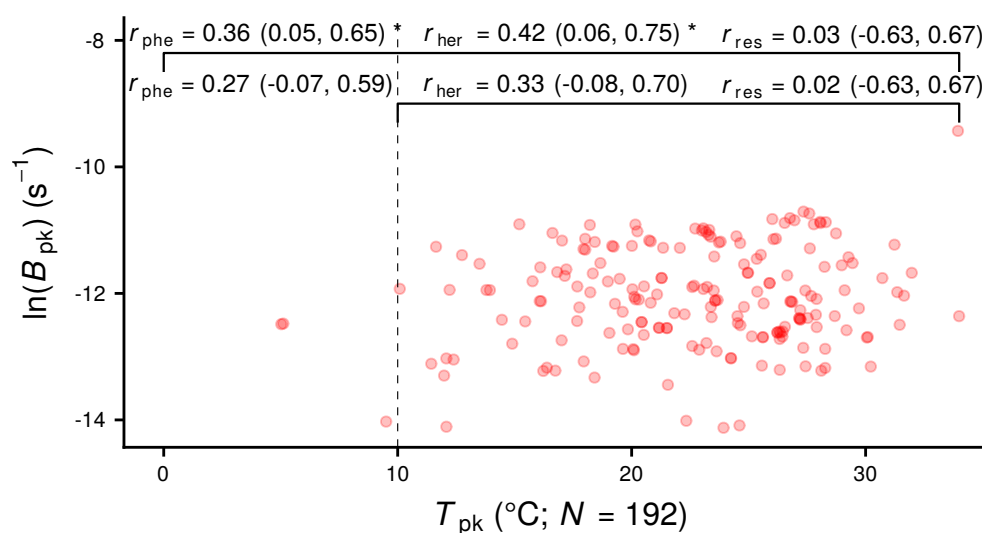


Figure 4. The environmentally and phylogenetically corrected relationship of T_{pk} with B_{pk} across the entire dataset, and after excluding data points with $T_{pk} < 10^\circ C$. r_{phe} , r_{her} , and r_{res} stand for phenotypic correlation, phylogenetically heritable correlation and residual correlation respectively. The correlations were estimated between $\ln(B_{pk})$ and T_{pk}^2 , but T_{pk} is shown in linear scale for simplicity. The values in parentheses correspond to the 95% HPD interval of each correlation coefficient.

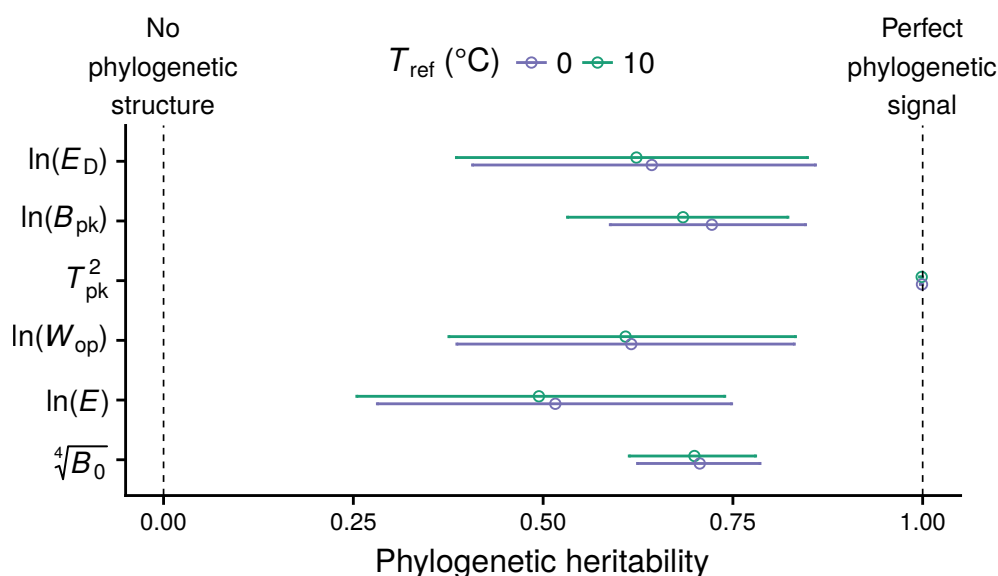


Figure 5. Phylogenetic heritability estimates across the TPC. Circles indicate the mean of the posterior distribution, whereas horizontal bars show the 95% HPD interval. Note that each TPC parameter was transformed towards approximate normality in order to satisfy the requirement of the MCMCglmm method.

(SI section S4.2). The only correlation that could be detected was between E and W_{op} (SI Fig. S23). The best-fitting model had a fixed effect of $\tilde{T}_{50m, 250d}$ (for $T_{ref} = 0^{\circ}\text{C}$; $R_m^2 = 0.445$ and $R_c^2 = 0.986$) or $\text{IQR}(T_{50m, 50d})$ (for $T_{ref} = 10^{\circ}\text{C}$; $R_m^2 = 0.463$ and $R_c^2 = 0.991$). More precisely, the analysis of all marine species revealed a negative relationship between $\ln(B_{pk})$ and the median temperature of trajectories at a depth of 50 meters and for a duration of 250 days ($\tilde{T}_{50m, 250d}$; SI Fig. S20). If, instead, only marine species with $T_{pk} > 10^{\circ}\text{C}$ are included, $\ln(E)$ is the parameter that associates with the environment, increasing with the interquartile range of temperatures of trajectories at a depth of 50 meters and for a duration of 50 days ($\text{IQR}(T_{50m, 50d})$; SI Fig. S22).

Size-scaling of growth rate

Cell volume-growth rate scaling—as predicted by the Metabolic Theory of Ecology and expected by the two hotter-is-better hypotheses—was detected only in the maximum height

of the curve (B_{pk} ; $R_m^2 = 0.15$ and $R_c^2 = 0.72$) and not at the performance at a temperature

of 0°C or 10°C ($R_m^2 = 0.00$ and $R_c^2 = 0.73$; SI Table S20 and SI Fig. S24). B_{pk} was found to scale with cell volume raised to an exponent of -0.1 (95% HPD interval = (-0.15, -0.05)).

The best-fitting models always had a random effect of species identity on the intercept and not the slope.

Discussion

In this study we investigated the influence of thermodynamic constraints on the shape of the thermal performance curve of phytoplankton (Fig. 2). To this end, we performed a thorough analysis of correlations among six TPC parameters. Controlling for the phylogeny of species and their local environment allowed us to better tease apart the relationships among thermal parameters, and quantify the influence of phylogeny on each TPC parameter.

As a first step, we examined the asymptotic correlations among the four main TPC parameters (B_0 , E , T_{pk} , and E_D) within each species' TPC to identify potential thermodynamic constraints. To the best of our knowledge, this approach has never been used before as a means of assessing the impact of thermodynamic constraints on TPC evolution. If hard thermodynamic constraints were generally in effect, certain TPC parameters would be expected to correlate strongly with each other, with very little variation in the correlation estimates across species. In other words, hard and ubiquitous thermodynamic constraints would necessarily lead to a nearly identical correlation structure across species, with large deviations from it being penalised by natural selection. In contrast, our analysis revealed a wide diversity of correlations among TPC parameter pairs. The only constraint that we could detect was a limit on the maximum height of the TPC (B_{pk}), indicated by a strong negative correlation between B_0 and E , found in most—but not all—TPCs. Such a tight coupling of B_0 and E suggests an equalisation of maximum performance across most species, achieved through adaptation. This pattern, along with the general lack of hard thermodynamic con-

straints, is inconsistent with the strict hotter-is-better hypothesis (Fig. 2). Therefore, we can rule out the strong thermodynamic constraints extreme of the spectrum as a possible location for phytoplankton TPCs.

The conclusions drawn from the previous analysis were well-supported by a phylogenetically- and environmentally-controlled investigation of correlations among all six TPC parameters. This additional analysis allowed us to detect a positive correlation between B_{pk} and T_{pk} (Fig. 4), which was however very weak and only held if TPCs with very low T_{pk} values were included. The only other detected correlation was between E and W_{op} (SI Fig. S17). The latter correlation is to be expected because niche width within the operational temperature range should vary inversely with thermal sensitivity (E). When focusing only on marine phytoplankton, we could detect neither a correlation between B_{pk} and T_{pk} , nor any correlation uniquely present in marine species. However, this may reflect the lower statistical power of the analysis of marine species due to the smaller sample size. In any case, as a correlation between B_{pk} and W_{op} was not detected in either the analysis of the entire dataset or in the analysis of correlations from marine species, the generalist-specialist tradeoff hypothesis can be rejected.

A single area of disagreement between the asymptotic (intraspecific) and the interspecific TPC correlations was the relationship between B_0 and E . While most TPCs had an intraspecific correlation of B_0 and E that was close to -1, such a correlation could not be detected across species ($r_{phe} = -0.05$; 95% HPD interval = (-0.23, 0.15)). This disagreement is most likely because of the low sample size of the analysis of intraspecific correlations. Perhaps a larger dataset would reveal the presence of TPCs with a slightly positive intraspecific correlation between B_0 and E ; this remains to be explored in future studies. Nevertheless, an interpretation of this result is that a coupling between B_0 and E (which could lead to an equalisation of B_{pk} across species) does occur in many TPCs, but it is not a hard constraint. In fact, this interpretation agrees nicely with the pattern shown in Fig. 4, where maximum performance is weakly dependent of temperature.

To fully narrow down the location of phytoplankton TPCs on the spectrum of hypotheses (Fig. 2), we examined i) the phylogenetic signal of all six TPC parameters, and ii) the effect of cell volume on growth rate. The phylogenetic signal estimates supported the rejection of the strict hotter-is-better hypothesis, which predicts a complete lack of phylogenetic signal in E . Nevertheless, the mean phylogenetic signal estimate of E was the lowest of all thermal parameters even if its posterior density interval was well above zero (Fig. 5). This result does not support a nearly constant E across species—as the MTE initially assumed (see Gillooly et al. 2001; Clarke and Fraser 2004; Clarke 2004; Gillooly et al. 2006; Clarke 2006)—, and provides some insight into the inter- and intraspecific variation in E reported by previous studies (e.g., Dell et al. 2011; Nilsson-Örtman et al. 2013; Pawar et al. 2016).

At the other end of the spectrum, the perfect biochemical adaptation hypothesis can also be rejected, as B_{pk} also exhibited phylogenetic signal. It is worth noting that the phylogenetic signal in B_{pk} does not merely reflect that the local environment is phylogenetically heritable (with closely related species occurring in geographically close environments), as the correlation between phylogenetic distance and geographical distance was almost zero (SI section S4.1). Finally, cell volume was found to weakly associate with the maximum height of the curve, and not with growth rate normalised at 0°C or 10°C. This association suggests an energetic tradeoff between cell volume and B_{pk} in phytoplankton. Based on this result, we hypothesize that the maintenance of a large cell volume should incur a high energetic cost, reducing the amount of energy that can be directed to cell growth. The weak negative scaling of B_{pk} with cell volume is consistent with our only remaining hypothesis: the weak hotter-is-better hypothesis. Indeed, given the weak correlations of i) B_{pk} with T_{pk} , and ii) B_{pk} with cell volume, an increase in T_{pk} would lead to a weak increase in B_{pk} and, indirectly, to a weak decrease in cell volume. Therefore, a decrease in cell size with warming—which has often been observed (Winder et al., 2009; Yvon-Durocher et al., 2011; Peter and Sommer, 2013; Sommer et al., 2017)—could be attributed to an indirect correlation between T_{pk} and cell volume.

We note that our results about the weak relationship between B_{pk} and T_{pk} , and the scaling of the former with cell volume are consistent with the conclusions of Kremer et al. (2017). They found evidence for the effects of temperature, taxonomic group, and cell size on the maximum growth rate of phytoplankton, effectively suggesting adaptation of B_{pk} across lineages. This further means that the classical Eppley curve (Eppley, 1972; Bissinger et al., 2008) does not necessarily indicate as strong a global (thermodynamic) constraint on maximum performance across species as has been previously thought. In this context, we also note that ideally cell size should be directly accounted for in analyses of TPC evolution. This was partially done in our study (i.e., by examining the relationship of cell volume with B_0 and B_{pk}), as we could not obtain cell volume measurements for all species in our dataset.

Thus, given all these results, we conclude that the TPCs of phytoplankton evolve in the general absence of hard thermodynamic constraints, similarly to the expectations of a very weak hotter-is-better hypothesis (Fig. 4). A possible mechanistic interpretation of the observed patterns is that, at very low temperatures, the limiting factor is low available kinetic energy, which constrains the rate of biochemical reactions. At higher temperatures, on the other hand, maximum trait performance appears temperature-independent, suggesting the presence of biophysical or other constraints. For example, given that B_{pk} scales negatively with cell volume, a lower limit in cell volume (e.g., due to the need for maintaining non-scalable cellular components such as membranes; Raven 1998) will also set an upper limit to the maximum possible growth rate. A thorough investigation of factors that constrain the maximum growth rate of phytoplankton at various temperatures could be the focus of future studies, as that would further our understanding of the limits to thermal adaptation.

Perhaps the most striking result of this study is that we detected a very limited number of correlations or tradeoffs across the entire TPC. One potential explanation for this could be that different phytoplankton lineages have evolved distinct strategies to maximise their fitness. Such strategies may involve thermal parameter correlations that are lineage-specific and hence hard to detect (see Fig. 3). A similar analysis performed separately for

each phytoplankton phylum could potentially address this question. However, obtaining accurate estimates of lineage-specific variance/covariance matrices of TPC parameters would require bigger thermal performance datasets than those that—to our knowledge—are currently available. It would also be interesting to investigate whether the phylogenetic signal of TPC parameters and the correlations among them vary across traits (e.g., photosynthesis rate, respiration rate) or phylogenetic groups (e.g., bacteria, plants). Such analyses could provide useful insights into the nature of possible constraints and their degree of influence on the shape of the thermal performance curve across different branches of the tree of life.

Another direction that could be further pursued involves investigating the effects of the marine environment on phytoplankton TPCs, and, in particular, how TPCs adapt to temperature fluctuations due to oceanic drifting (see e.g., Schaum et al. 2018). It is worth emphasising that, in our study, models that accounted for oceanic drifting of marine phytoplankton (models with Lagrangian variables) systematically performed better (in terms of DIC) than models that only incorporated the latitude or the sea surface temperature of the isolation locations of the strains. While we detected some associations between environmental variables and TPC parameters, the low sample size and the coarse modelling of drifting prevent us from drawing strong conclusions. More precisely, some of the limitations of our approach were that simulations were done at only three depths, and did not account for the vertical movement of phytoplankton or the concentration of nutrients. A more in-depth analysis on these matters could be the focus of future studies.

Conclusions

Our study sheds light on an ongoing debate regarding the influence of thermodynamics on the evolution of the TPC. Understanding this issue is key to predicting how climate change will impact ectotherm physiology and its knock-on effects on populations and communities. After controlling for potential phylogenetic and environmental effects, we find that thermo-

dynamic constraints have a limited impact on the shape of the TPC of growth rate among phytoplankton. In particular, most TPC parameters generally appear to evolve independently of each other, exhibiting a very weak hotter-is-better pattern. Overall, our results indicate that the thermal performance curve of phytoplankton evolves in the absence of hard thermodynamic constraints, and should thus have a strong potential for adaptation to vastly different thermal environments.

Author contributions

DGK and SP conceived and designed the study. DGK performed all analyses other than the simulations of marine phytoplankton trajectories, which were conducted by EvS and ML. DGK and SP interpreted the results. DGK wrote the initial manuscript, with comments and additions provided by all other coauthors.

Acknowledgements

We thank Bernardo García-Carreras and I. Colin Prentice for useful discussions and comments on an early version of the manuscript. We are also grateful to the CIPRES Science Gateway (Miller et al., 2010) and Imperial College London’s High Performance Computing service (doi:10.14469/hpc/2232) for access to computational resources. DGK was supported by a Natural Environment Research Council (NERC) Doctoral Training Partnership (DTP) scholarship (NE/L002515/1). SP and GYD were supported by NERC grants NE/M004740/1 and NE/M003205/1 respectively.

References

Aberer, A. J., K. Kobert, and A. Stamatakis. 2014. ExaBayes: massively parallel Bayesian tree inference for the whole-genome era. *Mol. Biol. Evol.* 31:2553–2556.

Angilletta, M. J. 2009. Thermal adaptation: a theoretical and empirical synthesis. Oxford
University Press.

Angilletta, M. J., R. B. Huey, and M. R. Frazier. 2009. Thermodynamic effects on organismal
performance: is hotter better? *Physiol. Biochem. Zool.* 83:197–206.

Banzon, V., T. M. Smith, T. M. Chin, C. Liu, and W. Hankins. 2016. A long-term record
of blended satellite and in situ sea-surface temperature for climate monitoring, modeling
and environmental studies. *Earth Syst. Sci. Data* 8:165–176.

Bissinger, J. E., D. J. S. Montagnes, J. Sharples, and D. Atkinson. 2008. Predicting marine
phytoplankton maximum growth rates from temperature: Improving on the Eppley curve
using quantile regression. *Limnol. Oceanogr.* 53:487–493.

Brooks, S. P., and A. Gelman. 1998. General methods for monitoring convergence of iterative
simulations. *J. Comput. Graph. Stat.* 7:434–455.

Brown, J. H., J. F. Gillooly, A. P. Allen, V. M. Savage, and G. B. West. 2004. Toward a
metabolic theory of ecology. *Ecology* 85:1771–1789.

Clarke, A. 2004. Is there a universal temperature dependence of metabolism? *Funct. Ecol.*
18:252–256.

———. 2006. Temperature and the metabolic theory of ecology. *Funct. Ecol.* 20:405–412.

———. 2017. *Principles of Thermal Ecology: Temperature, Energy, and Life*. Oxford
University Press.

Clarke, A., and K. Fraser. 2004. Why does metabolism scale with temperature? *Funct.*
Ecol. 18:243–251.

Dell, A. I., S. Pawar, and V. M. Savage. 2011. Systematic variation in the temperature
dependence of physiological and ecological traits. *Proc. Natl. Acad. Sci. U.S.A* 108:10591–
10596.

Doblin, M. A., and E. van Sebille. 2016. Drift in ocean currents impacts intergenerational
666 microbial exposure to temperature. *P. Natl. Acad. Sci. USA* 113:5700–5705.

Drummond, A. J., S. Y. Ho, M. J. Phillips, and A. Rambaut. 2006. Relaxed phylogenetics
and dating with confidence. *PLoS Biol.* 4:e88.

669 Eppley, R. W. 1972. Temperature and phytoplankton growth in the sea. *Fish. Bull.* 70:1063–
1085.

Falkowski, P., and J. Raven. 2013. *Aquatic Photosynthesis: Second Edition*. Princeton
672 University Press. URL <https://books.google.co.uk/books?id=kUCrAQAQAQBAJ>.

Field, C. B., M. J. Behrenfeld, J. T. Randerson, and P. Falkowski. 1998. Primary production
of the biosphere: integrating terrestrial and oceanic components. *Science* 281:237–240.

675 Flouri, T., and A. Stamatakis. 2012. An improvement to DPPDIV. Tech. rep. Heidel-
berg Institute for Theoretical Studies, Heidelberg, Germany, Exelixis-RRDR-2012-7. URL
<http://sco.h-its.org/exelixis/pubs/Exelixis-RRDR-2012-7.pdf>.

678 Frazier, M., R. B. Huey, and D. Berrigan. 2006. Thermodynamics constrains the evolution
of insect population growth rates: “warmer is better”. *Am. Nat.* 168:512–520.

Garamszegi, L. Z., and A. P. Møller. 2011. Nonrandom variation in within-species sample
681 size and missing data in phylogenetic comparative studies. *Syst. Biol.* 60:876–880.

García-Carreras, B., S. Sal, D. Padfield, D.-G. Kontopoulos, E. Bestion, C.-E. Schaum,
G. Yvon-Durocher, and S. Pawar. 2018. Role of carbon allocation efficiency in the tem-
684 perature dependence of autotroph growth rates. *Proc. Natl. Acad. Sci. U.S.A* P. 201800222.

Gelman, A., and D. B. Rubin. 1992. Inference from iterative simulation using multiple
sequences. *Stat. Sci.* 7:457–472.

687 Gillooly, J., A. Allen, V. Savage, E. Charnov, G. West, and J. Brown. 2006. Response to
Clarke and Fraser: effects of temperature on metabolic rate. *Funct. Ecol.* 20:400–404.

Gillooly, J. F., J. H. Brown, G. B. West, V. M. Savage, and E. L. Charnov. 2001. Effects of
size and temperature on metabolic rate. *Science* 293:2248–2251.

Global Names Architecture. 2017. Global Names Resolver. <http://resolver.globalnames.org/>. [Last accessed on December 7th, 2017].

Gu, X., Y.-X. Fu, and W.-H. Li. 1995. Maximum likelihood estimation of the heterogeneity
of substitution rate among nucleotide sites. *Mol. Biol. Evol.* 12:546–557.

Guindon, S., J.-F. Dufayard, V. Lefort, M. Anisimova, W. Hordijk, and O. Gascuel. 2010.
New algorithms and methods to estimate maximum-likelihood phylogenies: assessing the
performance of PhyML 3.0. *Syst. Biol.* 59:307–321.

Hadfield, J., and S. Nakagawa. 2010. General quantitative genetic methods for comparative
biology: phylogenies, taxonomies and multi-trait models for continuous and categorical
characters. *J. Evol. Biol.* 23:494–508.

Hadfield, J. D. 2010. MCMC Methods for Multi-Response Generalized Linear Mixed Models:
The MCMCglmm R Package. *J. Stat. Softw.* 33:1–22. URL <http://www.jstatsoft.org/v33/i02/>.

Heath, T. A., M. T. Holder, and J. P. Huelsenbeck. 2012. A Dirichlet process prior for
estimating lineage-specific substitution rates. *Mol. Biol. Evol.* 29:939–955.

Hinchliff, C. E., S. A. Smith, J. F. Allman, J. G. Burleigh, R. Chaudhary, L. M. Coghill,
K. A. Crandall, J. Deng, B. T. Drew, R. Gazis, K. Gude, D. S. Hibbett, L. A. Katz, H. D.
Laughinghouse, E. J. McTavish, P. E. Midford, C. L. Owen, R. H. Ree, J. A. Rees, D. E.
Soltis, T. Williams, and K. A. Cranston. 2015. Synthesis of phylogeny and taxonomy into
a comprehensive tree of life. *P. Natl. Acad. Sci. USA* 112:12764–12769.

Hochachka, P. W., and G. N. Somero. 2002. *Biochemical Adaptation: Mechanism and
Process in Physiological Evolution*. Oxford University Press.

Hoffmann, A. A., and C. M. Sgrò. 2011. Climate change and evolutionary adaptation. *Nature* 470:479–485.

Huey, R. B., and P. E. Hertz. 1984. Is a jack-of-all-temperatures a master of none? *Evolution* 38:441–444.

Jackson, C. H. 2011. Multi-State Models for Panel Data: The msm Package for R. *J. Stat. Softw.* 38:1–29. URL <http://www.jstatsoft.org/v38/i08/>.

Kamilar, J. M., and N. Cooper. 2013. Phylogenetic signal in primate behaviour, ecology and life history. *Philos. Trans. R. Soc. Lond., B, Biol. Sci.* 368:20120341.

Katoh, K., and D. M. Standley. 2013. MAFFT multiple sequence alignment software version 7: improvements in performance and usability. *Mol. Biol. Evol.* 30:772–780.

Knies, J. L., J. G. Kingsolver, and C. L. Burch. 2009. Hotter is better and broader: thermal sensitivity of fitness in a population of bacteriophages. *Am. Nat.* 173:419–430.

Kontopoulou, D. G., B. García-Carreras, S. Sal, T. P. Smith, and S. Pawar. 2018. Use and misuse of temperature normalisation in meta-analyses of thermal responses of biological traits. *PeerJ* 6:e4363.

Kremer, C. T., J. P. Gillette, L. G. Rudstam, P. Brettum, and R. Ptacnik. 2014. A compendium of cell and natural unit biovolumes for >1200 freshwater phytoplankton species. *Ecology* 95:2984–2984.

Kremer, C. T., M. K. Thomas, and E. Litchman. 2017. Temperature-and size-scaling of phytoplankton population growth rates: Reconciling the Eppley curve and the metabolic theory of ecology. *Limnol. Oceanogr.* 62:1658–1670.

Lange, M., and E. van Sebille. 2017. Parcels v0.9: prototyping a Lagrangian ocean analysis framework for the petascale age. *Geosci. Model. Dev.* 10:4175–4186. URL <https://www.geosci-model-dev.net/10/4175/2017/>.

López-Urrutia, Á., E. San Martín, R. P. Harris, and X. Irigoien. 2006. Scaling the metabolic
738 balance of the oceans. *P. Natl. Acad. Sci. USA* 103:8739–8744.

Masumoto, Y., H. Sasaki, T. Kagimoto, N. Komori, A. Ishida, Y. Sasai, T. Miyama, T. Mo-
741 toi, H. Mitsudera, K. Takahashi, H. Sakuma, and T. Yamagata. 2004. A fifty-year eddy-
resolving simulation of the world ocean: preliminary outcomes of OFES (OGCM for the
Earth Simulator). *J. Earth Simulator* 1:35–56.

Miller, M. A., W. Pfeiffer, and T. Schwartz. 2010. Creating the CIPRES Science Gateway
744 for inference of large phylogenetic trees. *in* Gateway Computing Environments Workshop
(GCE), 2010. Pp. 1–8. Ieee.

Morel, A., Y. Huot, B. Gentili, P. J. Werdell, S. B. Hooker, and B. A. Franz. 2007. Examining
747 the consistency of products derived from various ocean color sensors in open ocean (Case
1) waters in the perspective of a multi-sensor approach. *Remote Sens. Environ.* 111:69–88.

Morton, S. L., D. R. Norris, and J. W. Bomber. 1992. Effect of temperature, salinity and light
750 intensity on the growth and seasonality of toxic dinoflagellates associated with ciguatera.
J. Exp. Mar. Biol. Ecol. 157:79–90.

Nabhan, A. R., and I. N. Sarkar. 2012. The impact of taxon sampling on phylogenetic
753 inference: a review of two decades of controversy. *Brief. Bioinform.* 13:122–134.

Nakagawa, S., and R. P. Freckleton. 2008. Missing inaction: the dangers of ignoring missing
data. *Trends Ecol. Evol.* 23:592–596.

756 Nakagawa, S., and H. Schielzeth. 2013. A general and simple method for obtaining R^2 from
generalized linear mixed-effects models. *Methods Ecol. Evol.* 4:133–142.

Nilsson-Örtman, V., R. Stoks, M. De Block, H. Johansson, and F. Johansson. 2013. Lati-
759 tudinally structured variation in the temperature dependence of damselfly growth rates.
Ecol. Lett. 16:64–71.

Oehlert, G. W. 1992. A note on the delta method. *Am. Stat.* 46:27–29.

Padfield, D., C. Lowe, A. Buckling, R. Ffrench-Constant, S. Jennings, F. Shelley, J. S. Ólafsson, and G. Yvon-Durocher. 2017. Metabolic compensation constrains the temperature dependence of gross primary production. *Ecol. Lett.* 20:1250–1260.

Padfield, D., G. Yvon-Durocher, A. Buckling, S. Jennings, and G. Yvon-Durocher. 2016. Rapid evolution of metabolic traits explains thermal adaptation in phytoplankton. *Ecol. Lett.* 19:133–142.

Pagel, M. 1999. Inferring the historical patterns of biological evolution. *Nature* 401:877–884.

Parr, C. S., N. Wilson, P. Leary, K. S. Schulz, K. Lans, L. Walley, J. A. Hammock, A. Goddard, J. Rice, M. Studer, J. T. G. Holmes, and R. J. Corrigan. 2014. The Encyclopedia of Life v2: providing global access to knowledge about life on earth. *Biodivers. Data J.* .

Pawar, S., A. I. Dell, and V. M. Savage. 2015. From metabolic constraints on individuals to the dynamics of ecosystems. Pp. 3–36. *in* A. Belgrano, G. Woodward, and U. Jacob, eds. Aquatic Functional Biodiversity: An Ecological and Evolutionary Perspective. Elsevier.

Pawar, S., A. I. Dell, V. M. Savage, and J. L. Knies. 2016. Real versus artificial variation in the thermal sensitivity of biological traits. *Am. Nat.* 187:E41–E52.

Peter, K. H., and U. Sommer. 2013. Phytoplankton cell size reduction in response to warming mediated by nutrient limitation. *PLoS One* 8:e71528.

Pörtner, H. O., A. F. Bennett, F. Bozinovic, A. Clarke, M. A. Lardies, M. Lucassen, B. Pelter, F. Schiemer, and J. H. Stillman. 2006. Trade-offs in thermal adaptation: The need for a molecular to ecological integration. *Physiological and Biochemical Zoology* 79:295–313.

Rambaut, A., and A. J. Drummond. 2017. TreeAnnotator. <http://beast.community/treeannotator>. [Last accessed on November 7th, 2017].

Raven, J. 1998. The twelfth Tansley Lecture. Small is beautiful: the picophytoplankton. *Funct. Ecol.* 12:503–513.

Rose, J. M., and D. A. Caron. 2007. Does low temperature constrain the growth rates of heterotrophic protists? Evidence and implications for algal blooms in cold waters. *Limnol. Oceanogr.* 52:886–895.

Sal, S., L. Alonso-Sáez, J. Bueno, F. C. García, and Á. López-Urrutia. 2015. Thermal adaptation, phylogeny, and the unimodal size scaling of marine phytoplankton growth. *Limnol. Oceanogr.* 60:1212–1221.

Schaum, C.-E., A. Buckling, N. Smirnoff, D. Studholme, and G. Yvon-Durocher. 2018. Environmental fluctuations accelerate molecular evolution of thermal tolerance in a marine diatom. *Nat. Commun.* 9.

Schoolfield, R., P. Sharpe, and C. Magnuson. 1981. Non-linear regression of biological temperature-dependent rate models based on absolute reaction-rate theory. *J. Theor. Biol.* 88:719–731.

Sommer, U., K. H. Peter, S. Genitsaris, and M. Moustaka-Gouni. 2017. Do marine phytoplankton follow Bergmann’s rule *sensu lato*? *Biol. Rev.* 92:1011–1026.

Sørensen, J. G., C. R. White, G. A. Duffy, and S. L. Chown. 2018. A widespread thermodynamic effect, but maintenance of biological rates through space across life’s major domains. *bioRxiv* <https://www.biorxiv.org/content/early/2018/03/05/274944.full.pdf>.

Spiegelhalter, D. J., N. G. Best, B. P. Carlin, and A. van der Linde. 2002. Bayesian measures of model complexity and fit. *J. R. Stat. Soc. Series B Stat. Methodol.* 64:583–639.

Stamatakis, A. 2014. RAxML version 8: a tool for phylogenetic analysis and post-analysis of large phylogenies. *Bioinformatics* 30:1312–1313.

- 807 Symonds, M. R., and S. P. Blomberg. 2014. A primer on phylogenetic generalised least squares. Pp. 105–130. *in* Modern Phylogenetic Comparative Methods and Their Application in Evolutionary Biology: Concepts and Practice. Springer.
- 810 Tan, G., M. Muffato, C. Ledergerber, J. Herrero, N. Goldman, M. Gil, and C. Dessimoz. 2015. Current methods for automated filtering of multiple sequence alignments frequently worsen single-gene phylogenetic inference. *Syst. Biol.* 64:778–791.
- 813 Tavaré, S. 1986. Some probabilistic and statistical problems in the analysis of DNA sequences. Pp. 57–86. *in* R. M. Miura, ed. Some Mathematical Questions in Biology: DNA Sequence Analysis. American Mathematical Society, Providence (RI).
- 816 Thomas, M. K., C. T. Kremer, C. A. Klausmeier, and E. Litchman. 2012. A global pattern of thermal adaptation in marine phytoplankton. *Science* 338:1085–1088.
- de Villemereuil, P., and S. Nakagawa. 2014. General quantitative genetic methods for comparative biology. Pp. 287–303. *in* L. Z. Garamszegi, ed. Modern Phylogenetic Comparative Methods and Their Application in Evolutionary Biology: Concepts and Practice. Springer.
- 819 Wiens, J. J., and J. Tiu. 2012. Highly incomplete taxa can rescue phylogenetic analyses from the negative impacts of limited taxon sampling. *PLoS One* 7:e42925.
- Winder, M., J. E. Reuter, and S. G. Schladow. 2009. Lake warming favours small-sized planktonic diatom species. *Proc. R. Soc. Lond. B Biol. Sci.* 276:427–435.
- 825 Yvon-Durocher, G., J. M. Montoya, M. Trimmer, and G. Woodward. 2011. Warming alters the size spectrum and shifts the distribution of biomass in freshwater ecosystems. *Glob. Chang. Biol.* 17:1681–1694.